Hyperglycemia-Induced Thioredoxin-Interacting Protein Expression Differs in Breast Cancer–Derived Cells and Regulates Paclitaxel IC_{50}

Francesco Turturro,[1,2] Gary Von Burton,[1] and Ellen Friday[1,2]

Abstract

Purpose: We studied the hyperglycemia-induced expression of thioredoxin-interacting protein (TXNIP) expression and its relevance on the cytotoxic activity of paclitaxel in mammary epithelial–derived cell lines.

Experimental Design: Nontumorigenic cells (MCF10A); tumorigenic, nonmetastatic cells (MCF-7/T47D); and tumorigenic, metastatic cells (MDA-MB-231/MDA-MB-435s) were grown either in 5 or 20 mmol/L glucose chronically. Semiquantitative reverse transcription-PCR was used to assess TXNIP RNA expression in response to glucose. Reactive oxygen species were detected by CM-H2DCFDA (5-6-chloromethyl-2′,7′-dichlorodihydrofluorescein diacetate) and measured for mean fluorescence intensity with flow cytometry. Thioredoxin activity was assayed by the insulin disulfide-reducing assay. Proliferation was evaluated using CellTiter96 reagent with 490-nm absorption. Obtained absorbance values were used to calculate the paclitaxel IC_{50} in 5 or 20 mmol/L glucose using the Chou's dose-effect equation.

Results: We show that hyperglycemia by itself affects the level of TXNIP RNA in breast cancer–derived cells. TXNIP RNA level differs between nontumorigenic/nonmetastatic, tumorigenic cells (low TXNIP level), and metastatic cells (high TXNIP level). The differences in TXNIP RNA level, in reactive oxygen species level, and in thioredoxin activity are all related. We further show that hyperglycemia is a favorable condition in increasing the paclitaxel cytotoxicity by causing IC_{50} 3-fold decrease in metastatic breast cancer–derived MDA-MB-231 cells. The increased paclitaxel cytotoxicity is associated with an additive effect on the hyperglycemia-mediated TXNIP expression more evident in conditions of hyperglycemia than normoglycemia.

Conclusions: Our study opens a new perspective on the relevance of metabolic conditions of hyperglycemia in the biology and treatment of cancer, particularly in view of the epidemic of diabetes.

We have recently shown that the level of thioredoxin-interacting protein (TXNIP) RNA, also known as vitamin D_3 up-regulated protein-1, statistically significantly increased in response to levels of glucose shifted from 5 mmol/L (equivalent to metabolic condition of normoglycemia) to 20 mmol/L (equivalent to conditions of diabetes or postprandial hyperglycemia) in the highly metastatic breast cancer–derived MDA-MD-231 cells grown *in vitro* tissue culture (1). We also showed that TXNIP RNA level corresponded to persistent elevation of TXNIP protein (e.g., ref. 1).[3] Although increased TXNIP RNA level induced by hyperglycemia (20 mmol/L glucose) was associated with unchanged thioredoxin RNA level, thioredoxin measurable activity was notably reduced (1.6-fold than the control), and the level of reactive oxygen species (ROS) increased (2.3-fold than control), in MDA-MD-231 cells (1). We further showed that glucose-induced TXNIP/thioredoxin/ROS axis regulation was mediated by p38 mitogen-activated protein kinase (MAPK) signaling pathway because the use of SB203580-specific kinase inhibitor eliminated the glucose-induced effect on TXNIP and ROS (1). We also showed that the glucose transporter system (GLUT) is partially responsible for the glucose uptake–mediated effect on TXNIP regulation because this was notably, but not completely, reduced in the presence of GLUT1 inhibitor phloretin.[3] Our data favored the hypothesis that hyperglycemia increases the ROS level in cells responsive to the glucose-mediated up-regulation of TXNIP, and this effect may make the cells more vulnerable to oxidative damage. In fact, it has been well shown that

Authors' Affiliations: [1]Department of Medicine, Feist-Weiller Cancer Center and [2]Gene Therapy Program, Louisiana State University Health Science Center, Shreveport, Louisiana

Received 1/31/07; revised 3/19/07; accepted 3/22/07.

Grant support: NSF(2006)-Pfund-52 from the Board of Regents, Louisiana.

The costs of publication of this article were defrayed in part by the payment of page charges. This article must therefore be hereby marked *advertisement* in accordance with 18 U.S.C. Section 1734 solely to indicate this fact.

Requests for reprints: Francesco Turturro, Department of Medicine, Feist-Weiller Cancer Center, Louisiana State University Health Sciences Center, 1501 Kings Highway, Shreveport, LA 71103. Phone: 318-675-8863; Fax: 318-675-4338; E-mail: fturtu@lsuhsc.edu.

doi:10.1158/1078-0432.CCR-07-0244

[3] F. Turturro, E. Friday, and T. Welbourne, unpublished data.

hyperglycemia promotes oxidative stress through inhibition of thioredoxin by its binding due the formation of mixed cystein residue disulfide exchange with TXNIP in human aortic smooth muscle cells (2, 3). Based on observations from our group and from others, it seems that TXNIP acts as a modulator of the redox system through regulation of thioredoxin activity in various cell systems (2–5). The intracellular redox balance is maintained by ROS scavenger systems, mainly represented by the glutathione and the thioredoxin systems (6).

Diabetes and hyperglycemia are metabolic conditions in which DNA oxidative damage underlines the occurrence of complications of the disease as recently shown (7, 8). The emphasis on the role of both insulin and insulin-like growth factors or their binding proteins, together with the insulin-mediated regulation of fat distribution, availability of sex hormone binding globulin, and sex hormones in the regulation of proliferation and growth of breast-derived cells, has undermined the relevance of glucose by itself in breast cancer (9–12). In complex organisms, such as vertebrates, it becomes very difficult to discriminate glucose effects on gene transcription from those related to either insulin or glucagone, whose secretions are regulated by glucose (13). However, the use of established cell lines has allowed us in the previous study and in the current one to investigate the direct effect of glucose on regulation of the redox system in breast cancer–derived cell lines or in nonmalignant mammary epithelial–derived cell MCF10A (1). It has been shown that glucose consumption rate is lower in noninvasive MCF-7 cells versus metastatic breast cancer–derived MDA-MB-231 cells both in normoxic and hypoxic conditions (14). Gatenby et al. showed that up-regulation of glycolysis leads to microenvironmental acidosis as an evolutionary mechanism for the metastatic cell to adapt to the acidic microenvironment and promote proliferation and invasion (14). Although these authors have elegantly described this adaptive mechanism, the issue of how neoplastic cells react to hyperglycemia remains unsolved. A recent study of gene expression profile identified *TXNIP* as one of the redox signature genes that, when it is down-regulated, is associated with poor prognosis in patients with diffuse large B-cell lymphoma (15). Furthermore, earlier studies suggested that hyperglycemia may enhance the cytotoxicity of drugs in murine models of glioma and melanoma (16, 17). Finally, it has been recently shown that the histone deacytelase inhibitor suberoyalinide hydroxamic acid induced cell growth arrest through up-regulation of TXNIP in various cancer-derived cell lines (18).

Previous observations led us to ask the question whether hyperglycemia-regulated TXNIP/thioredoxin/ROS biology was a prerogative of metastatic MDA-MD-231 cells or more generally present in breast-derived cells with various phenotypes. Considering that paclitaxel (Taxol) is one of the chemotherapy agents used for treatment of breast cancer, we also wanted to explore whether this compound affected hyperglycemia TXNIP-mediated response and cell proliferation as an initial attempt in view of future screening of various chemotherapy agents with similar suberoyalinide hydroxamic acid effect on TXNIP. Our working hypothesis was that both the effect of hyperglycemia- and drug-induced TXNIP up-regulation would have made cancerous cells more susceptible to the antiproliferative effect of increased ROS levels.

Materials and Methods

Cell lines and tissue culture. Breast cancer–derived nontumorigenic MCF10A, nonmetastatic MCF-7/T47D, and metastatic MDA-MB-435s/MDA-MB-231 cells were purchased from the American Type Culture Collection. Cells were grown to confluence in DMEM plus 10% FCS containing 28 mmol/L sodium bicarbonate, 10 mmol/L sodium pyruvate, 5 mmol/L D-glucose, and 2 mmol/L L-glutamine at 37°C (pH 7.4). The cells were maintained in 5 or 20 mmol/L D-glucose chronically before plating.

Semiquantitative reverse transcription-PCR measurement of TXNIP RNA. Total RNA was isolated using Aquapure RNA isolation kit (Bio-Rad) and first-strand cDNA synthesis by iScript cDNA amplification kit (Bio-Rad) according to manufacturer's protocol. Primers were designed with Beacon Designer program (Premier Biosoft) as follows: TXNIP sense, 5′-TCATggTgATgtTCAAgAAgATC-3′ and antisense, 5′-ACTTCA-CACCTCCACTATC-3′; β-actin sense, 5′-TTTgAATgATgAgCCTTTgTg-3′ and antisense, 5′-TCAgTgTACAggTAAgCCCT-3′. PCR products for TXNIP and β-actin were amplified using PCR-Supermix (Promega) using 1:10 of the cDNA reaction mix with the following profile for 30 cycles: denaturation 95°C for 1 min, annealing 50°C for 1 min, and extension 68°C for 1 min. PCR products were run by electrophoresis on 3% agarose gel and stained with Syber-Sale DNA stain (Invitrogen). For semiquantization, amount of RNA was estimated by the relative intensity against the relative intensity of β-actin.

ROS assay and p38 MAPK inhibition. ROS was detected by CM-H2DCFDA (5-6-chloromethyl-2′,7′-dichlorodihydrofluorescein diacetate, acetyl ester; Molecular Probes) as previously described (2). Briefly, cells were loaded with 10 μmol/L DCFDA for 30 min at 37°C, 5% CO_2 in PBS. Cells were washed and returned to media for a 30-min recovery period. Mean fluorescence intensity was used as a measure of ROS as determined by flow cytometry FACSCalibur using CellQuest Pro 5.2 (BD Biosciences; ref. 6). For p38 MAPK inhibition experiments, cells were initially maintained in 5 or 20 mmol/L glucose media, and then the cells at 20 mmol/L glucose were treated for 24 h with 20 μmol/L specific inhibitor SB203580 (Sigma).

Quantitative analysis of dose-effect relationship between paclitaxel and glucose. Cells were plated in 96-well dishes at ~3,000 per well and allowed to attach and spread overnight before drug treatment. At time 0, media with 5 or 20 mmol/L glucose and various concentrations of paclitaxel were added, and plates were incubated for 24 h. Proliferation was evaluated using CellTiter96 reagent (Promega). Briefly, 20 μL of reagent was added to each well, and plates were returned to incubator for an additional 2 h for color development. Absorption at 490 nm was measured on ThermoMax microplate reader (Molecular Devices) with SoftmaxPro 4.3 software. The obtained absorbance values were used to calculate the IC_{50} of paclitaxel in 5 or 20 mmol/L glucose using the Chou's dose-effect equation as described elsewhere (19). Contrarily to the Chou's original method, we analyzed the effects of multiple concentrations of glucose on the drug instead of analyzing the effects of multiple drugs in terms of summation, synergism, or antagonism as described (15).

Statistical analysis. All the experiments were carried in triplicates. Differences between treatments were evaluated by ANOVA or Student's t test. Differences were accepted as significant if $P < 0.05$.

Results

TXNIP RNA response to hyperglycemia differs in mammary epithelial–derived nonmalignant/nonmetastatic cells versus metastatic cells. We have previously shown that the level of TXNIP RNA message statistically significantly increases from 5 to 20 mmol/L glucose in metastatic breast cancer–derived cells MDA-MB-231 (1). In that study, we showed that the TXNIP RNA increased within 6 h after acute exposure to 20 mmol/L

(condition of post-prandial hyperglycemia) and remained elevated in condition of chronic elevation of the glucose in the media (hyperglycemia/diabetes). To assess whether the response of TXNIP to hyperglycemia is a general mechanism present in breast epithelial–derived cells or limited to metastatic breast cancer–derived cells, we investigated this response in nontumorigenic mammary epithelial cells (MCF10A); in nonmetastatic, tumorigenic mammary epithelial cells (MCF7 and T47D); and finally in metastatic, tumorigenic mammary epithelial cells (MDA-MB-435s and MDA-MB-231). As shown in Fig. 1A, the fold-increase compared with β-actin of TXNIP RNA as determined by reverse transcription-PCR was modest, considering individually MCF10A (1.3 ± 0.2), MCF-7 (1.1 ± 0.2), or T47D cells (1.3 ± 0.04), compared with higher fold increase in MDA-MB-435s (2.5 ± 0.1) and MDA-MB-231 cells (4.7 ± 0.5). Clearly, the nontumorigenic/tumorigenic, nonmetastatic cells as a group (1.2 ± 0.15; Fig. 1A, *inset, low*) presented statistically significant lower fold increase ($P < 0.04$) of TXNIP RNA versus metastatic cells (3.6 ± 0.67; Fig. 1A, *inset, high*). Our data show that TXNIP RNA is responsive to hyperglycemia regulation differently in nontumorigenic/tumorigenic, nonmetastatic breast cancer–derived cells compared with metastatic-derived cells, with the latter being more sensitive to the level of glucose.

ROS levels and thioredoxin activity are affected differently by hyperglycemia-regulated TXNIP in mammary epithelial–derived cells. It has been recently shown that TXNIP binds to thioredoxin and modulates its activity as a major cellular redox regulator (2, 3). We have recently shown that hyperglycemia-induced TXNIP RNA elevation is associated with decreased thioredoxin activity without changes in thioredoxin RNA level, resulting in increasing levels of ROS in MDA-MB-231 cells (1). To assess whether the difference in hyperglycemia-regulated TXNIP RNA levels previously described was associated with differences in ROS level/thioredoxin activity, we studied them in the same group of cell lines. As shown in Fig. 2A, ROS levels detected by CMH2DCFDA and expressed as fold increase of the percentage of mean fluorescence compared with control (20 versus 5 mmol/L glucose) increased less in tumorigenic, nonmetastatic cells [MCF-7 (1.08 ± 0.02) and T47D (1.24 ± 0.03)] and in nontumorigenic cells [MCF10A (1.54 ± 0.03)] in response to hyperglycemia than in metastatic, tumorigenic cells [MDA-MB-435s (1.88 ± 0.06) or MDA-MB-231 (2.34 ± 0.25)]. In fact, when the cells were grouped in low/TXNIP level (MCF-7/T47D/MCF10A, 1.29 ± 0.21) versus high/TXNIP level (MDA-MB-435s/MDA-MB-231, 2.11 ± 0.13), the difference in ROS levels was statistically significantly different between the two groups (Fig. 2A, *inset*; $P < 0.05$). On the other hand, Fig. 2B shows that the decrease of thioredoxin activity measured as described, and expressed as fold decrease compared with control (20 versus 5 mmol/L glucose), was less pronounced in nontumorigenic cells [MCF10A (1.21 ± 0.01)] and tumorigenic, nonmetastatic cells [MCF-7 (1.25 ± 0.02) and T47D (1.38 ± 0.09)] compared with metastatic cells [MDA-MB-435s (1.57 ± 0.17) and MDA-MB-231 (1.6 ± 0.13)]. When the cells were grouped in low level (MCF10A/MCF-7/T47D, 1.28 ±

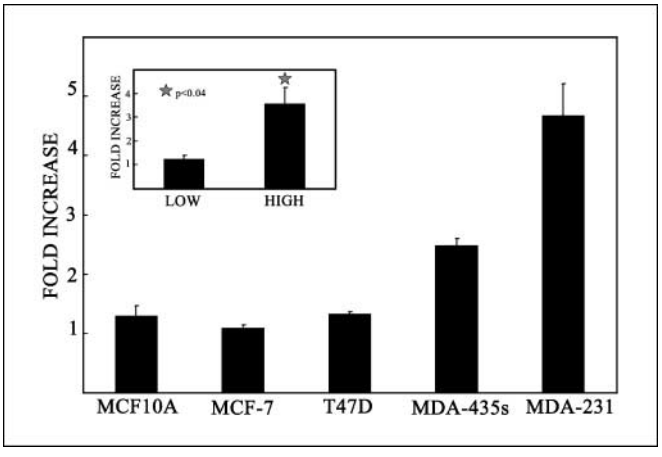

Fig. 1. TXNIP RNA response to hyperglycemia in mammary epithelial – derived nonmalignant/nonmetastatic cells versus metastatic cells. Cells were grown either in 5 or 20 mmol/L glucose chronically before plating. TXNIP RNA message levels were detected by semiquantitative PCR in all cells grown in the same conditions as specified. Average fold increase compared with control β-actin RNA of TXNIP RNA messages from triplicates are represented for each individual cell line or by grouping in low level (MCF10A/MCF-7/T47D) and high level (MDA-MB-231/MDA-MB-435s) of expression (*inset*).

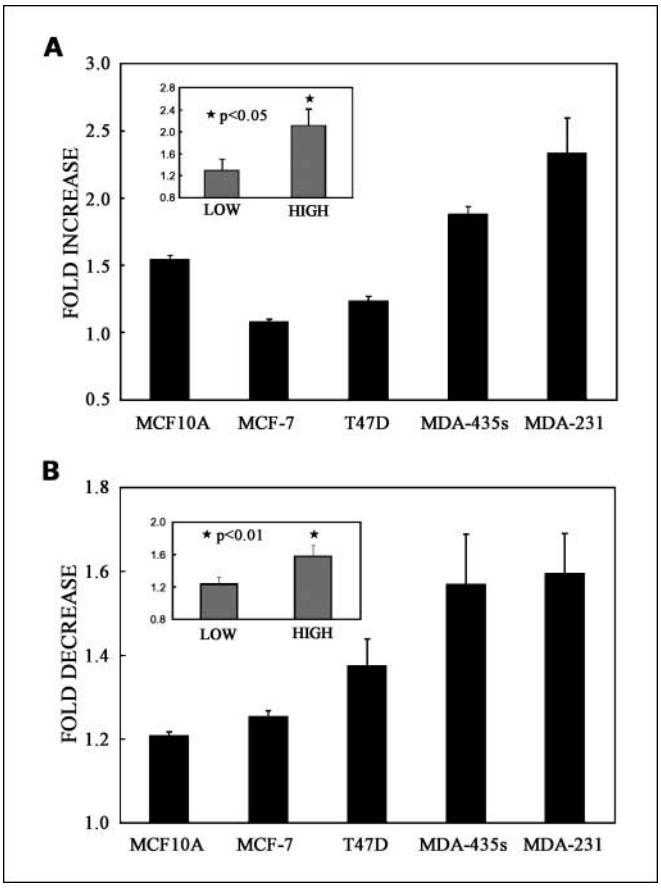

Fig. 2. *A,* ROS level in response to hyperglycemia in mammary epithelial – derived nonmalignant/nonmetastatic cells versus metastatic cells. Cells were grown either in 5 or 20 mmol/L glucose chronically before plating. Cells were assessed for ROS levels by DCFDA fluorescence staining and flow cytometry. Average fold increase of mean fluorescence from triplicates is expressed for each individual cell line or by grouping in low level (MCF10A/MCF-7/T47D) and high level (MDA-MB-231/MDA-MB-435s) of TXNIP expression (*inset*). *B,* thioredoxin activity in response to hyperglycemia in mammary epithelial – derived nonmalignant/nonmetastatic cells versus metastatic cells. Cells were grown either in 5 or 20 mmol/L glucose chronically before plating. Cells were assessed for thioredoxin activity by the insulin disulfide-reducing assay as described, the average A_{410} readings, and expressed as fold decrease compared to controls in triplicates for each individual cell line or by grouping in low level (MCF10A/MCF-7/T47D) and high level (MDA-MB-231/MDA-MB-435s) of TXNIP expression (*inset*).

0.09) versus high level (MDA-MB-435s/MDA-MD-231, 1.58 ± 0.13) of TXNIP RNA expression, the difference in thioredoxin activity was statistically significantly different in favor of the TXNIP/high level, metastatic group ($P < 0.01$). These data show that metastatic breast cancer cells are more responsive to hyperglycemia-induced TXNIP regulation of the thioredoxin/ROS axis, as shown by increased ROS production compared with nontumorigenic or tumorigenic, nonmetastatic cells. This effect may reflect a general down-regulation of the TXNIP responsive mechanism (blunt response) to hyperglycemia in the latter compared with the former.

Hyperglycemia reduces the IC_{50} of paclitaxel in MDA-MD-231 cells. We then asked the question whether metabolic conditions of hyperglycemia have any consequences on the response of metastatic cells MDA-MB-231 to paclitaxel, a chemotherapy agent used in the treatment of breast cancer. For this purpose, we studied the effect of various concentrations of paclitaxel on the proliferation of MDA-MB-231 cells grown in both concentrations of 5 and 20 mmol/L glucose media. As shown in Fig. 3A, the number of cells grown at 20 mmol/L and expressed as A_{490} was statistically significantly higher than those grown at 5 mmol/L glucose [time 0: 0.67 ± 0.01 ($n = 5$) versus 0.82 ± 0.02 ($n = 20$); $P = 0.005$] as expected for being more proliferative in media with higher glucose content. A_{490} declined dramatically as an index of decreased proliferation with the increasing dose of the drug, being more prominent in cells grown at 20 versus 5 mmol/L glucose [20 nmol/L paclitaxel: 5 versus 20 mmol/L glucose, $P = 0{,}003$ (Fig. 3A); 0.63 nmol/L: 0.64 ± 0.01 ($n = 5$) versus 0.79 ± 0.02 ($n = 20$); 1.25 nmol/L: 0.61 ± 0.005 ($n = 5$) versus 0.71 ± 0.04 ($n = 20$); 2.5 nmol/L: 0.61 ± 0.01 ($n = 5$) versus 0.58 ± 0.03 ($n = 20$); 5 nmol/L: 0.59 ± 0.01 ($n = 5$) versus 0.46 ± 0.02 ($n = 20$); 10 nmol/L: 0.55 ± 0.02 ($n = 5$) versus 0.39 ± 0.01 ($n = 20$); 20 nmol/L: 0.53 ± 0.01 ($n = 5$) versus 0.35 ± 0.004 ($n = 20$; Fig. 3A)]. On the other hand, if we considered the percentage of treated cell death (compared with untreated control) as shown in Fig. 3B, the cytotoxic effect of the drug became progressively more evident between 5 versus 20 mmol/L glucose media, starting reaching statistically significant difference at concentration of 2.5 nmol/L paclitaxel [0.63 nmol/L: 3.4 ± 0.67 ($n = 5$) versus 3 ± 2.4 ($n = 20$); 1.25 nmol/L: 6.4 ± 0.46 ($n = 5$) versus 10.9 ± 4.3 ($n = 20$); 2.5 nmol/L: 6.5 ± 1.2 ($n = 5$) versus 24.58 ± 2.8 ($n = 20$); 5 nmol/L: 7.6 ± 0.81 ($n = 5$) versus 26.3 ± 2 ($n = 20$); 10 nmol/L: 11.7 ± 2.2 ($n = 5$) versus 43.5 ± 0.7 ($n = 20$); 20 nmol/L: 14.3 ± 1.3 ($n = 5$) versus 47.4 ± 0.3 ($n = 20$)]. When we ultimately considered the logarithmic conversion and linear regression by plotting the logarithmic (LOG) ratio of the values of the fraction of affected cells (f_A)/fraction of unaffected cells (f_U) versus logarithm of dose (LOG_D) as shown in Fig. 3C, we were able to show that IC_{50} of paclitaxel decreased one third from 33 nmol/L at 5 mmol/L glucose to 10 nmol/L at 20 mmol/L glucose. These data clearly showed that hyperglycemia favors proliferation, but the metabolic condition made MDA-MB-231 cells more susceptible to the cytotoxic effect of the chemotherapy agent paclitaxel.

Hyperglycemia/TXNIP/ROS correlates with TXNIP RNA level. Based on the observation that hyperglycemia sensitizes the cytotoxic effect of paclitaxel in MDA-MB-231 cells, we investigated whether TXNIP/ROS axis was involved in this response. To this end, we decided to use the dose of paclitaxel (20 nmol/L) that had the highest cytotoxic effect in the previous set of experiments (Fig. 3A and B). The level of TXNIP RNA did not change in cells grown at 5 mmol/L glucose and treated with paclitaxel for 24 h (Fig. 4A: 5/control 1.0 ± 0.2 versus 5/paclitaxel 0.8 ± 0.2, $P = 0.68$). On the contrary, TXNIP RNA level that already statistically significantly increased with 20 mmol/L glucose compared with 5 mmol/L glucose control (Fig. 4A: 1.5 ± 0.1, $P < 0.01$) and further increased compared with 20 mmol/L glucose control after 24-h treatment with

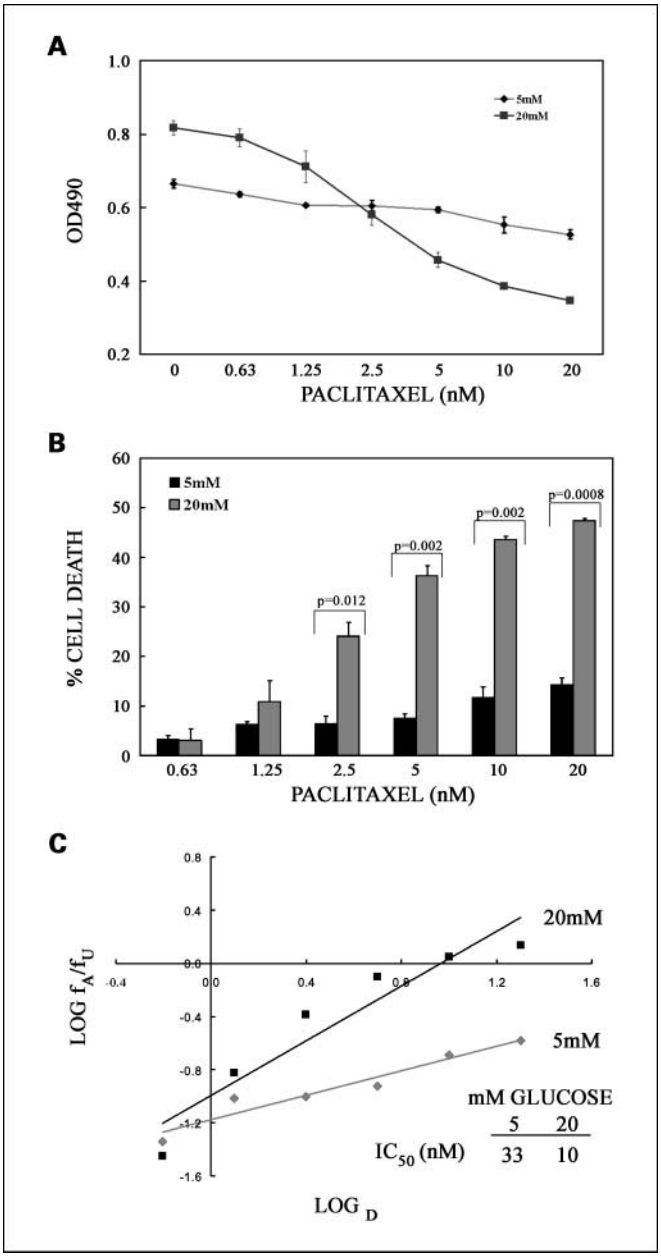

Fig. 3. *A,* MDA-MB-231 cell proliferation. Cells were plated in 96-well dishes at ~3,000 per well, allowed to attach, and treated as specified in Materials and Methods. Average of triplicates at various concentrations of glucose and paclitaxel. *B,* MDA-MB-231 percentage of cell death. Cells were treated as in (*A*). Triplicates of the percentage of dead cells in the treated group versus matched untreated controls with the statistically significant different *P* of the paired groups. *C,* obtained absorbance values were used to calculate the IC_{50} of paclitaxel in 5 or 20 mmol/L glucose using the Chou's dose-effect equation as described elsewhere (15). Values of logarithm (LOG) of the ratio of fraction of affected cells (f_A)/fraction of unaffected cells (f_U) plotted versus logarithm of dose (LOG_D).

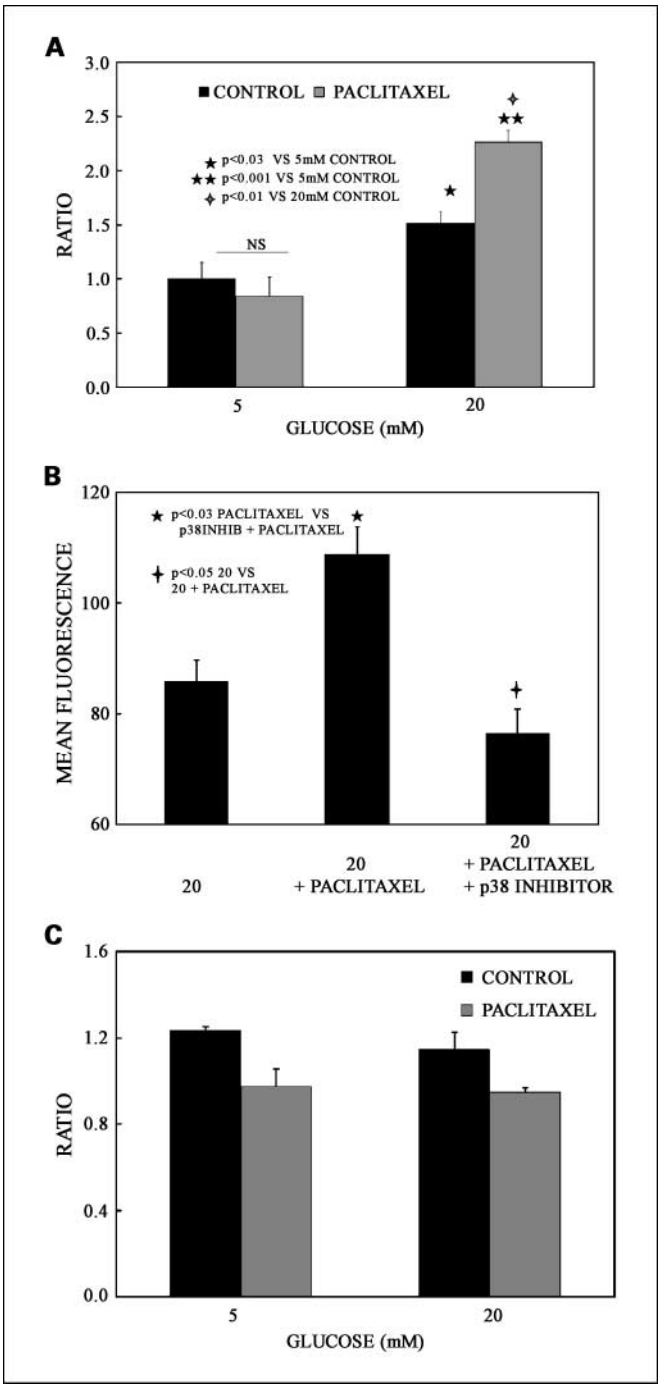

Fig. 4. *A,* TXNIP RNA response to hyperglycemia and paclitaxel in MDA-MB-231 cells. Cells were grown either in 5 or 20 mmol/L glucose chronically with and without 20 nmol/L paclitaxel. TXNIP RNA message levels were detected by semiquantitative PCR in all cells grown in the same conditions as specified. Average ratio of relative levels compared with control β-actin RNA of TXNIP RNA messages from triplicates are represented for each group of cells. *B,* ROS level in response to hyperglycemia, paclitaxel, and p38 MAPK inhibitor in MDA-MB-231 cells. ROS was detected by CM-H2DCFDA as described. Average mean fluorescence from triplicate experiments. For p38 MAPK inhibition experiments, cells were maintained in 20 mmol/L glucose media and then treated for 24 h with 20 μmol/L specific inhibitor SB203580. *C,* TXNIP RNA response to hyperglycemia and paclitaxel in MCF-7 cells. Cells were grown and treated as in (*A*). TXNIP RNA message levels were detected by semiquantitative PCR in all cells grown in the same conditions as specified. Average ratio of the relative levels compared with control β-actin RNA of TXNIP RNA messages from triplicates are represented for each group of cells.

paclitaxel (Fig. 4A: 2.3 ± 0.1, $P < 0.01$). These data show that paclitaxel has an additive effect on the regulation of TXNIP RNA levels present only in condition of hyperglycemia compared with normal levels of glucose in MDA-MB-231 cells.

To assess whether the increased level of TXNIP resulting from the additive effect of hyperglycemia + paclitaxel was associated with concurrent increased ROS, we measured ROS levels in MDA-MB-231 cells grown in 20 mmol/L with/without 20 nmol/L paclitaxel for 24 h. As shown in Fig. 4B, the level of ROS was further elevated by paclitaxel [86 ± 4 (20 mmol/L glucose) versus 109 ± 5 (20 mmol/L glucose + 20 nmol/L paclitaxel), $P < 0.05$]. Because a recent study has shown that hyperglycemia-induced increased level of TXNIP is associated with activation of p38 MAPK in human aortic smooth muscle cells, we assessed whether the p38 MAPK signaling pathway was also involved in the paclitaxel-induced TXNIP/ROS up-regulation (6). For this purpose, we treated MDA-MD-231 cells with 20 μmol/L of the specific kinase inhibitor SB203580. As illustrated in Fig. 4B, the inhibition of p38 MAPK reversed completely the paclitaxel-induced elevation of ROS level [76 ± 3 (20 mmol/L glucose + 20 nmol/L paclitaxel + SB203580), $P < 0.03$ (Fig. 4B)]. These findings indicate that paclitaxel magnifies the hyperglycemia-induced regulation of TXNIP-ROS in MDA-MB-231 cells, and this effect is mediated through the p38 MAPK signaling pathway. Finally, we assessed whether nonmetastatic, tumorigenic MCF-7 cells presented the same response to paclitaxel in terms of TXNIP RNA levels independently from glucose regulation of TXNIP because we already showed that the response to hyperglycemia was blunt in these cells (Fig. 1). Surprisingly, as shown in Fig. 4C, paclitaxel did not elevate TXNIP levels in condition of hyperglycemia after 24 h of treatment as occurred in MDA-MB-231 cells in the same experimental conditions [1.24 ± 0.01 (5 mmol/L glucose) versus 0.98 ± 0.08 (5 mmol/L glucose + paclitaxel), $P = 0.104$; 1.15 ± 0.08 (20 mmol/L glucose) versus 0.95 ± 0.02 (20 mmol/L glucose + paclitaxel), $P = 0.17$]. These data confirm that the TXNIP-ROS hyperglycemia + paclitaxel effect is both cell dependent and related to the hyperglycemia-induced TXNIP regulation through p38 MAPK signaling pathway. In other words, cells not responding to hyperglycemia in terms of regulation of TXNIP/ROS present a blunt response to both glucose and paclitaxel.

Discussion

In this study, we show that the metabolic condition of hyperglycemia by itself affects the level of TXNIP RNA in breast cancer–derived cells. The level of TXNIP RNA differs between nontumorigenic/nonmetastatic, tumorigenic cells (low TXNIP level), and metastatic cells (high TXNIP level). The difference in TXNIP RNA level is associated with differences in ROS levels and thioredoxin activity. In fact, the low TXNIP RNA level group (MCF10A/MCF-7/T47D cells) presents statistically significantly lower fold increase of ROS levels compared with the high TXNIP RNA level group (MDA-MB-435s/MDA-MB-231 cells). This condition is further associated with statistical significant difference in the fold decrease of thioredoxin activity in these two groups of cells being lower in the former compared with the latter. In our cellular model, we have reproduced the conditions of post-prandial hyperglycemia by shifting the glucose level from 5 to 20 mmol/L and the conditions of

insulin-resistant hyperglycemia (diabetes) by maintaining the cells "chronically" at 20 mmol/L glucose. In the current study, we show that these metabolic conditions have a major effect on both the level of TXNIP and the regulation of ROS level/thioredoxin activity in metastatic cells but not in nontumorigenic/nonmetastatic, tumorigenic cells. More recently, we and others have shown by gene expression profile analysis that TXNIP presents an exquisite sensitivity to glucose levels in metastatic breast cancer–derived cells MDA-MB-231 and in murine pancreatic β cells, respectively (1, 20). The same group of investigators showed that the promoter region of the *TXNIP* gene contains carbohydrate-responsive elements that confers the described responsiveness in murine pancreatic β cells (21). As depicted in Fig. 5, considering that TXNIP inhibits thioredoxin activity, and its level is highly regulated by glucose uptake, we suggest that this protein may play a major role in translating the biological consequences of a metabolic condition, such as hyperglycemia/diabetes, in regulating the response of breast cancer cells to a situation of oxidative stress associated with this condition. Recent studies have related the effect of hyperglycemia to increased generation of ROS and to greater DNA oxidative damage as the main mechanism of accelerated aging and atherogenesis in the microangiopathic complications of the disease (2, 8). Although the relevance of diabetes in the pathogenesis and clinical course of tumors in general and particularly of breast cancer has been controversially debated, we provide for the first time the molecular relationship among hyperglycemia, TXNIP, and increased ROS production occurring in an *in vitro* cellular model simulating diabetic conditions (9).

As shown in Figs. 1 and 2, the order of magnitude of the glucose-induced TXNIP/ROS regulation decreases with the progression of the malignant phenotype. Hence, the magnitude of the glucose-induced *TXNIP* gene expression, and consequently its mechanism of regulation rather than the TXNIP level, seems to be associated with the metastatic phenotype particularly in MDA-MB-231 cells. These findings were unexpected because malignant cells highly depend upon glycolysis, and the question whether hyperglycemia-induced TXNIP represents a favorable or an unfavorable function remains unanswered (14, 22). Although various studies have recently addressed the relevance of TXNIP in cancer biology, our study is the first one relating it to hyperglycemia/diabetes. In fact, a recent study has shown that the expression of TXNIP assessed by immunohistochemistry in cells from colon/gastric primary tumor tissues is reduced compared with adjacent normal tissue from the primary tissue of the tumors (23). Other studies have shown that the loss of TXNIP expression may be involved in human T-cell lymphotrophic virus-1–induced lymphoproliferative transformation, or as co-repressor suppresses interleukin-3 receptor and cyclin A2 promoter activity functioning (24, 25). Furthermore, it seems that TXNIP may regulate cell growth by increasing the stability of $p27^{kip1}$ (26). Finally, it has recently been shown that exogenous expression of TXNIP suppresses tumor growth in breast cancer–derived cells MCF-7 and is responsible for the formation of metastases in melanoma (27, 28).

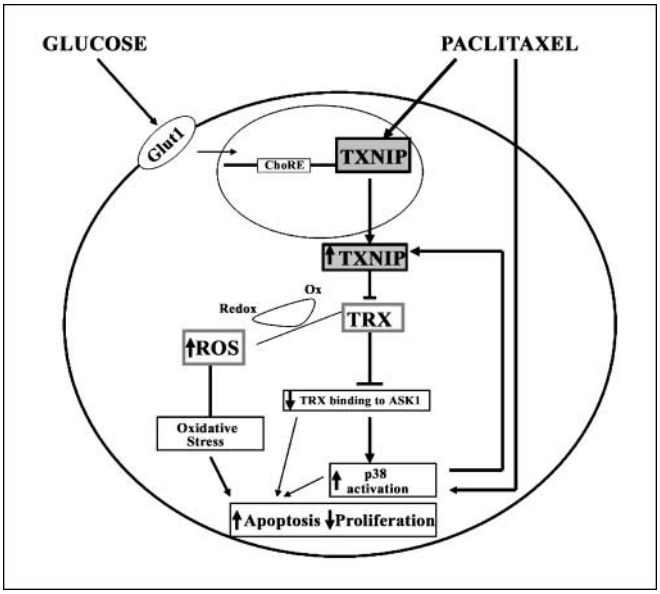

Fig. 5. Hyperglycemia-mediated regulation of the TXNIP/thioredoxin (*TRX*)/ROS axis in inducing oxidative stress and paclitaxel-mediated additive effect in the cellular model. GLUT-mediated glucose uptake regulates the *TXNIP* gene expression through the carbohydrate response elements (*ChoRE*) as previously shown (21). The increased level of TXNIP RNA is associated with reduced thioredoxin activity and increased ROS levels. This mechanism has been well elucidated and involves p38 MAPK signaling pathway as shown by our group and by Schulze et al. (1, 2). Paclitaxel increases the hyperglycemia-induced elevation of TXNIP RNA level and magnifies the ROS-mediated oxidative stress – negative effect on cell proliferation as shown in the current study. The inhibition of p38 MAPK signaling pathways hampers this effect.

Although it has been recently shown that both 5-fluorouracil and histone deacetylase inhibitor suberoylanilide hydroxamic acid induce TXNIP expression, none of these studies addressed the relevance of glucose in this action (24, 29). Definitively, our study favors the idea that TXNIP renders cancerous cells more susceptible to oxidative stress (Fig. 5). Although it has been proven that overexpression of TXNIP suppresses growth and induces apoptosis in vascular smooth muscle cells and cardiomyocytes, it has only been more recently that apoptosis and "glucotoxicity" have been related through increased glucose-regulated endogenous TXNIP expression in murine pancreatic β cells (21, 30–33). However, in the current study, we did not investigate the ultimate effect of hyperglycemia-mediated TXNIP expression on apoptosis. Hitherto, we addressed the issue on the consequences that this mechanism may have on drug response. We show that hyperglycemia favors the cytotoxicity of paclitaxel and causes a 3-fold decrease of IC_{50} in metastatic breast cancer–derived MDA-MB-231 cells. The increased paclitaxel cytotoxicity is associated with an additive effect on the hyperglycemia-mediated TXNIP expression, which is only evident in conditions of elevated glucose and absent in conditions of normoglycemia (Fig. 5). The direct consequence of this effect yields increased production of ROS in our study. Previous studies have underlined the ROS-mediated induction of apoptosis as mechanism of cytotoxicity for paclitaxel (34–36). More recently, studies have identified increased level of thioredoxin as a mechanism of resistance to docetaxel, a taxane similar to paclitaxel used for chemotherapy of breast cancer (37, 38). As shown in Fig. 5, our data favor a role for p38 MAPK signaling pathway in the regulation of the hyperglycemia/paclitaxel–mediated TXNIP expression. We and others have previously shown that p38 MAPK affects the hyperglycemia-mediated regulation of TXNIP (1, 2). On the other hand, p38 MAPK may also be a downstream signaling pathway involved in both TXNIP response and paclitaxel direct effect (Fig. 5). In fact, it has been shown that TXNIP down-regulation by using RNA interference increases the association

of thioredoxin with a partner kinase ASK-1, causing the inhibition of the activation of p38 MAPK and c-Jun NH_2-terminal kinase signaling pathways and ultimately apoptosis in endothelial cells (39). It has also been shown that paclitaxel induces apoptosis through p38 MAPK–dependent inhibition of the Na^+/H^+ exchanger 1 in metastatic breast cancer–derived cells MDA-MB-435 (40). None of the previous studies though had shown a relationship between glucose-TXNIP and paclitaxel. Ultimately, we cannot exclude that the proliferative effect of glucose increases the number of mitosis and favors the binding of paclitaxel to β-tubulin of the mitotic spindle, which is considered the major mechanism of the taxane-induced growth arrest of tumor cells at the G_2-M phase (41).

In conclusion, in an era when the "epidemic of diabetes," a major concern for the health of the future generations in the United States, has been dominating the attention of the media and the public health care providers, our study opens new perspectives and questions on the relevance of metabolic conditions of hyperglycemia in the biology and treatment of cancer.[4] Particularly, in view of the hypothesis that hyperglycemia may favor the cytotoxicity of certain drugs with similar suberoylanilide hydroxamic acid–mediated effects on TXNIP, the availability of compounds, such as 3-*O*-methylglucose, that stimulate TXNIP expression without being metabolized through phosphorylation by glucokinase, makes it attractive in terms of combining it with such drugs in preclinical animal models (42, 43).

[4] Pollan M. Unhappy meals (New York Times visited on Jan. 30, 2007; http://www.nytimes.com/2007/01/28/magazine/28nutritionism.t.html).

References

1. Turturro F, Friday E, Ye G, et al. Role of hyperglycemia-induced thioredoxin-interacting protein (TXNIP) in metastatic breast cancer [abstract 429]. Proc AACR 2006;47.
2. Schulze PC, Yoshioka J, Takahashi T, et al. Hyperglycemia promotes oxidative stress through inhibition of thioredoxin function by thioredoxin-interacting protein. J Biol Chem 2004;279:30369–74.
3. Patwari P, Higgins LJ, Chutkow WA, Yoshioka J, Lee RT. The interaction of thioredoxin with Txnip. J Biol Chem 2006;281:21884–91.
4. Nishiyama A, Matsui M, Iwata S, et al. Identification of thioredoxin-binding protein-2/vitamin D(3) up-regulated protein 1 as a negative regulator of thioredoxin function and expression. J Biol Chem 1999; 274:21645–50.
5. Junn E, Han SH, Im JY, et al. Vitamin D3 up-regulated protein 1 mediates oxidative stress via suppressing the thioredoxin function. J Immunol 2000;164:6287–95.
6. Yamawaki H, Berk BC. Thioredoxin: a multifunctional antioxidant enzyme in kidney, heart and vessels. Curr Opin Nephrol Hypertens 2005;14:149–53.
7. Nishikawa T, Edelstein D, Du XL, et al. normalizing mitochondrial superoxide production blocks three pathways of hyperglycemic damage. Nature 2000; 404:787–90.
8. Dandona P, Thusu K, Cook S, et al. Oxidative damage to DNA in diabetes mellitus. Lancet 1996;347:444–5.
9. Muti P. The role of endogenous hormone in the etiology and prevention of breast cancer: the epidemiologic evidence. Ann N Y Acad Sci 2004;1028:273–82.
10. Milazzo G, Giorgino F, Damante F, et al. Insulin receptor expression and function in human breast cancer cell lines. Cancer Res 1992;52:3924–30.
11. Cullen KJ, Yee D, Sly WS, et al. Insulin-like growth factor receptor expression and function in human breast cancer. Cancer Res 1990;50:48–53.
12. Cara JF. Insulin-like growth factors, insulin-like growth factor binding proteins and ovarian androgen production. Horm Res 1994;42:49–54.
13. Lefrancois-Martinez AM, Martinez A, Antoine B, Raymondjean M, Kahn A. Upstream stimulatory factor proteins are major components of the glucose response complex of the L-type pyruvate kinase gene promoter. J Biol Chem 1995;270:2640–3.
14. Gatenby RA, Gillies RJ. Why do cancers have high aerobic glycolysis? Nat Rev Cancer 2004;4:891–9.
15. Tome ME, Johnson DBF, Rimsza LM, et al. A redox signature score identifies diffuse large B-cell lymphoma patients with a poor prognosis. Blood 2005;106: 3594–601.
16. Schem BC, Roszinski S, Krossnes BK, Mella O. Timing of hypertonic glucose and thermochemotherapy with 1-(4-amino-2-methylpyrimidine-5-yl)methyl-3-(2-chloroethyl)-3-nitrosurea (ACNU) in the BT_4An rat glioma: relation to intratumoral pH reduction and circulatory changes after glucose supply. Int J Radiat Oncol Biol Phys 1995;33:409–16.
17. Canter RJ, Zhou R, Kesmodel SB, et al. Metaiodobenzylguanidine and hyperglycemia augment tumor response to isolated limb perfusion in a rodent model of human melanoma. Ann Surg Oncol 2004;11:265–73.
18. Butler LM, Zhou X, Xu WS, et al. The histone deacetylase inhibitor SAHA arrests cancer cell growth, up-regulates thioredoxin-binding protein-2, and down-regulates thioredoxin. Proc Natl Acad Sci U S A 2002;99:11700–5.
19. Chou TC, Talalay P. Quantitative analysis of dose-effect relationships: the combined effects of multiple drugs of enzyme inhibitors. Adv Enzyme Regul 1984; 22:27–55.
20. Shalev A, Pise-Masison CA, Radonovich M, et al. Oligonucleotide microarray analysis of intact human pancreatic islets: identification of glucose-responsive genes and a highly regulated TGFbeta signaling pathway. Endocrinology 2002;143:3695–8.
21. Minn AH, Hafele C, Shalev A. Thioredoxin-interacting protein is stimulated by glucose through a carbohydrate response element and induces beta-cell apoptosis. Endocrinology 2005;146:2397–405.
22. Beckner ME, Stracke ML, Liotta LA, Schiffmann E. Glycolysis as primary energy source in tumor cell chemotaxis. J Natl Cancer Inst 1990;82:1836–40.
23. Ikarashi M, Takahashi Y, Yshii Y, Nagata T, Assai S, Ishikawa K. Vitamin D3 up-regulated protein 1 (VDUP1) expression in gastrointestinal cancer and its relation to stage of disease. Anticancer Res 2002;22:4045–8.
24. Han SH, Jeon JH, Ju HR, et al. VDUP1 upregulated by TGF-beta1 and 1,25-dihydroxyvitamin D_3 inhibits tumor cell growth by blocking cell-cycle progression. Oncogene 2003;22:4035–46.
25. Nishinaka Y, Nishiyama A, Masutani H, et al. Loss of thioredoxin-binding protein-2/vitamin D3 up-regulated protein 1 in human T-cell leukemia virus type I-dependent T-cell transformation: implications for adult T-cell leukemia leukemogenesis. Cancer Res 2004;64:1287–92.
26. Jeon JH, Lee KN, Hwang CH, Kwon KS, You KH, Choi I. Tumor suppressor VDUP1 increases p27 (kip1) stability by inhibiting JAB1. Cancer Res 2005;65: 4485–9.
27. Nishinaka Y, Masutani H, Oka S, et al. Importin alpha1 (Rch1) mediates nuclear translocation of thioredoxin-binding protein-2/vitamin D(3)-up-regulated protein 1. J Biol Chem 2004;279:37559–65.
28. Goldberg SF, Miele ME, Hatta N, et al. Melanoma metastasis suppression by chromosome 6: evidence for a pathway regulated by CRSP3 and TXNIP. Cancer Res 2003;63:432–40.
29. Takahashi Y, Nagata T, Ishii Y, Ikarashi M, Ishikawa K, Asai S. Up-regulation of vitamin D_3 up-regulated protein 1 gene in response to 5-fluorouracil in colon carcinoma SW620. Oncol Rep 2002;9:75–9.
30. Yoshioka J, Schreiter ER, Lee RT. Role of thioredoxin in cell growth through interactions with signaling molecules. Antioxid Redox Signal 2006;8:2143–51.
31. Schulze PC, De Keulenaer GW, Yoshioka J, Kassik KA, Lee RT. Vitamin D_3 up-regulated protein 1 (VDUP1) regulates redox-dependent vascular smooth muscle cell proliferation through interaction with thioredoxin. Circ Res 2002;91:689–95.
32. Wang Y, De Keulenaer GW, Lee RT. Vitamin D(3)-upregulated protein-1 is a stress-responsive gene that regulates cardiomyocyte viability through interaction with thioredoxin. J Biol Chem 2002;277:26496–500.
33. World CJ, Yamawaki H, Berk BC. Thioredoxin in the cardiovascular system. J Mol Med 2006;84:997–1003.
34. Pae HO, Jun CD, Yoo JC, et al. Enhancing and priming of macrophages for superoxide anion production by taxol. Immunopharmacol Immunotoxicol 1998;20: 27–37.
35. Wang Y, Chen C, Chung S, et al. Involvement of oxidative stress and caspase activation in paclitaxel-induced apoptosis of primary effusion lymphoma cells. Cancer Chemother Pharmacol 2004;54:322–30.
36. Park S, Wu C, Gordon JD, Zhong X, Emami A, Safa AR. Taxol induces caspase-10-dependent apoptosis. J Biol Chem 2004;279:51057–67.
37. Koizumi K, Matoba R, Ueno N, et al. Prediction of docetaxel response in human breast cancer by gene expression profiling. J Clin Oncol 2005;23:422–31.
38. Kim SJ, Miyoshi Y, Taguchi T, et al. High thioredoxin expression is associated with resistance to docetaxel in primary breast cancer. Clin Cancer Res 2005;11: 8425–30.
39. Yamawaki H, Pan S, Lee RT, Berk BC. Fluid shear stress inhibits vascular inflammation by decreasing thioredoxin-interacting protein in endothelial cells. J Clin Invest 2005;115:733–8.
40. Reshkin SJ, Bellizzi A, Cardone RA, Tommasino M, Casavola V, Paradiso A. Paclitaxel induces apoptosis via protein kinase A- and p38 mitogen-activated protein-dependent inhibition of the Na^+/H^+ exchanger (NHE) NHE isoform 1 in human breast cancer cells. Clin Cancer Res 2003;9:2366–73.
41. Crown J, O'Leary M. The taxanes: an update. Lancet 2000;355:1176–8.
42. Minn AH, Cuoto FM, Shalev A. Metabolism-independent sugar effects on gene transcription: the role of 3-*O*-methylglucose. Biochemistry 2006;45: 11047–51.
43. Ahsan MK, Masutani H, Yamguchi Y, et al. Loss of interleukin-2-dependency in HTLV-1-infected T cells on gene silencing of thioredoxin-binding protein-2. Oncogene 2006;25:2181–91.